POWER ATTENUATION OF MARTIAN ROVERS AND LANDERS SOLAR PANELS DUE TO DUST DEPOSITION.

T. Pierron, F. Forget, E. Millour, *Laboratoire de Météorologie Dynamique (LMD), IPSL, Sorbonne Université, CNRS, Paris, France, (thomas.pierron@lmd.ipsl.fr)*.

Introduction

Because of the high amount of dust in the Martian atmosphere, solar panels of landers and rovers on Mars are covered by the dust in the course of their mission. This accumulation makes available power significantly decrease over the sols. During most missions, winds were able to blow the dust away. These "dust cleaning events", as they are called, are followed by an increase of the electrical current produced by the solar arrays. In order to better predict the amount of available power by solar panels in the Martian conditions, a model of dust accumulation was developed into the existing LMD Mars 1D thermal model, a radiative convective model derived from a full 3D General Circulation Model. This dust accumulation model, which takes into account a full radiative transfer in the atmosphere and in the dust layer accumulated on the panel, gives a good approximation of the power loss due to dust accumulation on flat or inclined surfaces, such as solar panels.

Design of dust accumulation model

To have the best approximation of the amount of dust accumulated on a surface, one must know with the best precision the speed at which the dust accumulates on solar panels. The dust deposition rate R_{dust} (in kg.m^{-2}.s^{-1}) in LMD1D is computed as follows :

$$R_{\text{dust}} = mmr \times \rho \times W_{\text{s}} \qquad (1)$$

with mmr the mass mixing ratio of the dust near the surface, ρ the dust density and W_{s} the Stokes speed at which the dust falls. The latter is computed with the formula from *Rossow* (1978) [6].

The mass mixing ratio is a function of the dust opacity τ of the atmosphere, the single scattering extinction coefficient Q_{ext} and the surface pressure P_{surf} :

$$mmr = \frac{4}{3}\frac{\rho r_{\text{eff}}\tau}{Q_{\text{ext}}}\frac{g}{P_{\text{surf}}} \qquad (2)$$

Consequently, having the best model for dust opacity in the atmosphere is essential to know the amount of dust accumulated on the solar panels. This is why full dust scenarios were added to the LMD1D model. These scenarios, one for each Martian Year (MY) from MY24 to MY35 (described in *Montabone et al.* (2015) [4] and *Montabone et al.* (2020) [5]), are based on observations

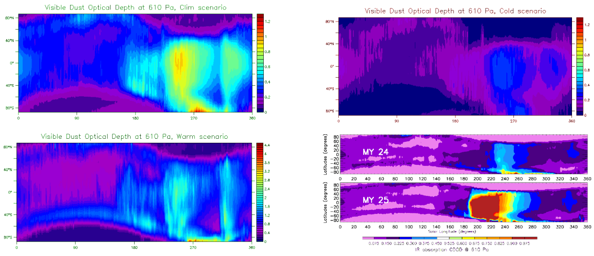

Figure 1: Visible ($0.67\mu m$) extinction column dust optical depth at 610Pa as a function of latitude (ordinate) and solar longitude (abscissa), longitudinally averaged for Climatology, Cold and Warm scenario. Infrared absorption ($9.3\mu m$) column dust optical depth at 610Pa for MY24/25 scenarios. Climatology scenario in the top left-hand corner, Cold scenario in the top right-hand corner, Warm Scenario in the bottom left-hand corner and MY24/25 scenario in the bottom right-hand corner. Plots are shown at different scales in order to see the variations; from *Montabone et al.* (2015-2020) [4]- [5]

from April 1999 to today and contain daily values (over 669 sols of a Martian year) of infrared (9.3 μm) absorption column dust optical depth at 610Pa, with a horizontal resolution of $5°$ in longitude x $5°$ in latitude. This opacity is converted to the extinction optical depth in the visible (0.67 μm) and is used in equation (2). The conversion coefficients values are discussed in *Smith* (2004) [7] and *Wolff and Clancy* (2003) [11]. Figures 1 shows different scenrarios, the climatology scenario, representative of a standard year in terms of dust, the cold scenario corresponding to an extremely clear atmosphere and the warm scenario, which corresponds to a very "dusty" atmosphere. Scenarios corresponding to specific Martian Years (MY) are also avalaible in the model, MY24 and MY25 are shown as an example.

At each time step, the dust deposition rate is integrated to calculate the total mass of dust which has been accumulated since the beginning of the run :

$$M_{\text{dust}} = \int_0^t R_{\text{dust}}(t')\,\mathrm{d}t' \qquad (3)$$

.

Then, this mass is used to compute the opacity of the accumulated dust layer τ_{acc} :

$$\tau_{\text{acc}} = \frac{3M_{\text{dust}}Q_{\text{ext}}}{4\rho r_{\text{acc}}} \qquad (4)$$

where r_{acc} is the effective radius of the dust particles deposited on the panel. This opacity will be used by the radiative transfer model, the 2-stream multiple scattering scheme, presented in *Toon et al.* (1989) [10], to compute the solar flux under the dust layer, the solar flux above the dust layer being computed with the model of *Spiga and Forget* (2008) [8], taking into account the local slope of the surface on which the dust has accumulated. Other parameters such as the single scattering albedo of dust particle, the asymmetry parameter of the dust which characterises the direction where the light will be scattered, the solar zenith angle on the slope and the albedo of the solar panel are also taken into account.

Validation of the model

The model, described previously, was compared to the solar arrays data measured by different missions on Mars. The electrical current was directly available for Insight missions so the comparison was almost direct. Given that the model gives the solar flux (in $W.m^{-2}$) while the observations are electrical current (in A), it was assumed a proportionnal relation between the two variables. The proportionnality coefficient remains the same for all the simulation and is computed using the maximum electrical current at the beggining of the mission, when the panels are not dusty yet, and the solar flux received by the panel under the dust layer calculated by the model. Figure 2 shows the comparison between the model and the observation for maximum daily current, for different values of accumulated dust particles radius r_{acc}. The best effective radius to fit Insight data seem to be $r_{\text{acc}} = 7$ μm and was the one used for other comparisons. In order to evaluate the diurnal cycle of the solar flux, we also compared the model with the Insight measurements over a few days with several values per day. This also allows to check the effect of the solar zenith angle. The comparison is shown on Figure 3.

For the MER missions, only the dust factor which represents the attenuation coefficient due to accumulated dust is available to us so far. Therefore the comparison between these data and the LMD1D model is not totally consistent. The results are still presented here in Figures 4 and 5. The model gives a good overall fit for long term variations of the dust factor, even if for Spirit it underestimates a little the dust factor. Moreover, given the large duration of the MER missions, some cleaning events were observed during the missions. Therefore, these cleaning events were simulated starting a new simulation after each cleaning event, with the amount of dust corresponding to the dust factor reported at this exact same date.

The Pathfinder mission happended in MY23 and dust scenarios are only available from MY24. However the observations of current show that MY23 was a dusty year. Therefore the model was used with MY27 which was also very dusty. The comparison with the dust fac-

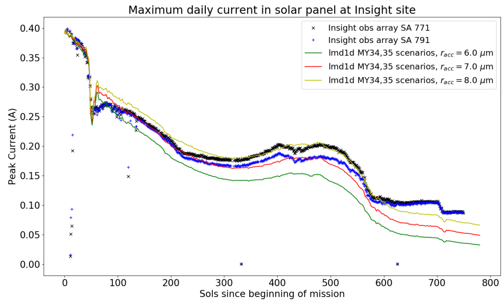

Figure 2: Maximum daily current (in A) measured by the two solar panels (blue for SA791, black for SA771) of Insight over time (sols). Isolated measurements are simply because measurements were not acquired at noon. The solid lines correspond to LMD1D with different effective radius for accumulated dust : 6 μm in green, 7 μm in red, 8 μm in yellow. An effective radius of 7 μm gives the best fit. The measurements are taken from *Lorenz et al.* (2020) [3]

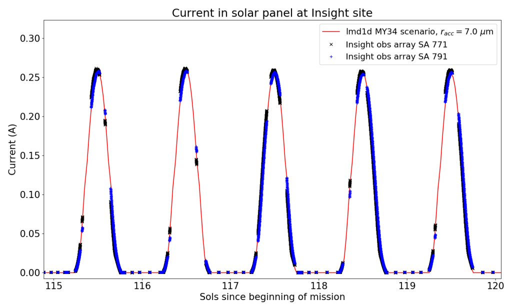

Figure 3: Current (in A) measured by the two solar panels (blue for SA791, black for SA771) of Insight over time (sols). One can see that the current is maximum at noon and null during night. The measurements are taken from *Lorenz et al.* (2020) [3]

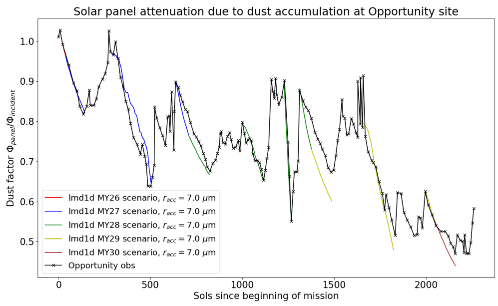

Figure 4: Maximum daily dust factor measured by Opportunity over time (sols). The coloured solid lines correspond to LMD1D model with the appropriate scenarios. The measurements are taken from *Stella and Herman* (2010) [9]

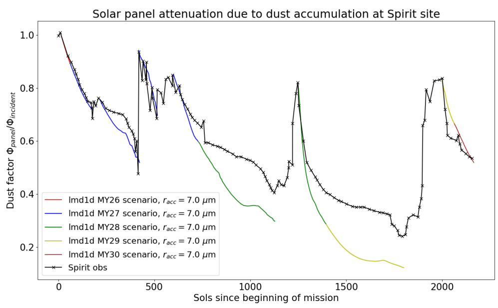

Figure 5: Maximum daily dust factor measured by Spirit over time (sols). The coloured solid lines correspond to LMD1D model with the appropriate scenarios. The measurements are taken from *Stella and Herman* (2010) [9]

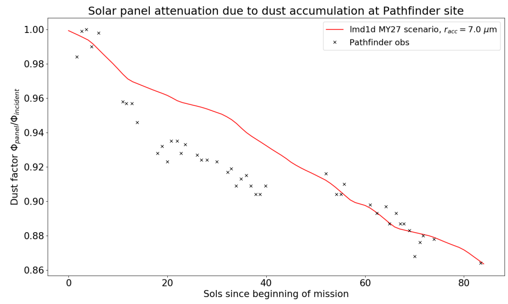

Figure 6: Maximum daily dust factor measured by Pathfinder over time (sols). The solid line in red corresponds to LMD1D model with the MY27 scenario. The measurements are taken from *Crisp et al.* (2004) [1]

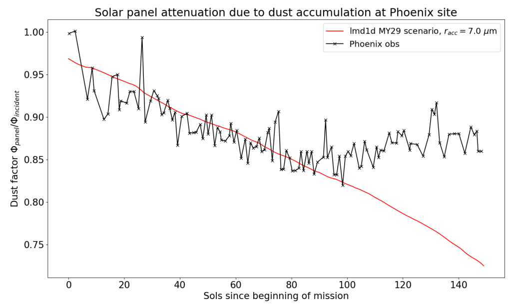

Figure 7: Maximum daily dust factor measured by Phoenix over time (sols). The solid red line corresponds to LMD1D model with the MY29 scenario. The simulation starts with a dust factor of 0.97 to simulate the dust lifted during the landing. The solid line in black correspond to the observations done by Phoenix solar panel. The measurements are taken from *Drube et al.* (2010) [2].

tor, shown on Figure 6, gives a good fit overall even if locally, some gaps between the model and the measurements are observed.

Dust factor from Phoenix electrical current data was also compared to the model. It was chosen to start the simulation with a dust factor of 0.97 to simulate the large amount of dust that might have been lifted and redeposited during and after the landing, as explained in *Drube et al.* (2010) [2]. The comparison is presented on Figure 7. After sol 100, as we can see, the dust factor generally goes back up, likely due to a dust cleaning event, which are not simulated by the model.

Summary

This new tool included in the updated version of the LMD1D model allows to have a good prediction of the surface power in W.m^{-2} received by a surface such as a solar panel. The inclination and the orientation of the panel are taken into account in the model and can be precised as inputs of the model. However, the model does not take into account any dust cleaning events which makes it pessimistic and therefore, a good tool for future missions.

References

[1] David Crisp, Asmin Pathare, and RC Ewell. The performance of gallium arsenide/germanium solar cells at the martian surface. *Acta Astronautica*, 54(2):83–101, 2004.

[2] Line Drube, Kristoffer Leer, W Goetz, Haraldur Pall Gunnlaugsson, Martin Patrong Haspang, N Lauritsen, MB Madsen, LKD Sørensen, MD Ellehoj, MT Lemmon, et al. Magnetic and optical properties of airborne dust and settling rates of dust at the phoenix landing site. *Journal of Geophysical Research: Planets*, 115(E5), 2010.

[3] Ralph D Lorenz, Mark T Lemmon, Justin Maki, Donald Banfield, Aymeric Spiga, Constantinos Charalambous, Elizabeth Barrett, Jennifer A Herman, Brett T White, Samuel Pasco, et al. Scientific observations with the insight solar arrays: Dust, clouds, and eclipses on mars. *Earth and Space Science*, 7(5):e2019EA000992, 2020.

[4] L Montabone, F Forget, E Millour, RJ Wilson, SR Lewis, B Cantor, D Kass, A Kleinböhl, MT Lemmon, MD Smith, et al. Eight-year climatology of dust optical depth on mars. *Icarus*, 251:65–95, 2015.

[5] Luca Montabone, Aymeric Spiga, David M Kass, Armin Kleinböhl, François Forget, and Ehouarn Millour. Martian year 34 column dust climatology from mars climate sounder observations: Reconstructed maps and model simulations. *Journal of Geophysical Research: Planets*, page e2019JE006111, 2020.

[6] William B Rossow. Cloud microphysics: Analysis of the clouds of earth, venus, mars and jupiter. *icarus*, 36(1):1–50, 1978.

[7] Michael D Smith. Interannual variability in tes atmospheric observations of mars during 1999–2003. *Icarus*, 167(1):148–165, 2004.

[8] Aymeric Spiga and François Forget. Fast and accurate estimation of solar irradiance on martian slopes. *Geophysical research letters*, 35(15), 2008.

[9] Paul M Stella and Jennifer A Herman. The mars surface environment and solar array performance. In *2010 35th IEEE Photovoltaic Specialists Conference*, pages 002631–002635. IEEE, 2010.

[10] Owen B Toon, CP McKay, TP Ackerman, and K Santhanam. Rapid calculation of radiative heating rates and photodissociation rates in inhomogeneous multiple scattering atmospheres. *Journal of Geophysical Research: Atmospheres*, 94(D13):16287–16301, 1989.

[11] Michael J Wolff and R Todd Clancy. Constraints on the size of martian aerosols from thermal emission spectrometer observations. *Journal of Geophysical Research: Planets*, 108(E9), 2003.